

# Prediction of Land Cover Compliance to the Drought Frequency under Climate Change Conditions in Hemrin Watershed

Mahmoud Saleh Al-Khafaji<sup>1\*</sup>, Rusul Abdul Hadi Al-Ameri<sup>2</sup>, Fouad H. Saeed<sup>3</sup>

<sup>1</sup>Department of Civil Engineering, Al-Nahrain University, Baghdad, Iraq

<sup>2</sup>Department of Civil Engineering, University of Technology, Baghdad, Iraq

<sup>3</sup>Ministry of Water Resources, Iraq

\*Corresponding author's email : [mahmoud.s.al-khafaji@ced.nahrainuniv.edu.iq](mailto:mahmoud.s.al-khafaji@ced.nahrainuniv.edu.iq)

## Abstract

Climate change plays a crucial role in the frequency of extreme climate events, which greatly impacts the status of land cover (LC). In this paper, the compliance of LC to the drought frequency patterns (DFPs) was assessed for the present and future conditions in Hemrin Watershed, Iraq. The Climate Forecast System Reanalysis (CFSR) data were used in the analysis of monthly weather data and the Reconnaissance Drought Index (RDI) of Hemrin Watershed for the period 1984-2013. In addition, a satellite-based analysis of the vegetation cover (VC) was conducted. Consequently, the satellite-based VC and DFPs were compared to investigate the effect of DFPs on VC and the trend of VC. The results indicated that drought was dominant in the last decades with two or three dry years followed by one wet year. Furthermore, the VC decreased by 0.5% and 4.5% during the dry and wet seasons respectively. The VC can be recovered when consecutive dry years are followed by two or more consecutive wet years and the drought frequency is reduced by 23% and 28% during dry and wet seasons respectively. However, when the wet years are dominant and successive, VC increases by 1% and 37% during dry and wet seasons respectively. The watershed is sensitive to climate change and the VC is highly related to the drought frequency. The dry area is expected to increase to cover most of the watershed by 2049 due to climate change consequents. The seasonal drought needs more investigation in future studies.

**Keywords:** Land Cover, Drought frequency, Climate Change, Hemrin.

## تخمين تماثل الغطاء الأرضي مع تردد الجفاف تحت ظروف التغير بالمناخ في جابية حميرين

محمود صالح الخفاجي<sup>1\*</sup>, رسل عبد الهادي العامري<sup>2</sup>, فواد حسين

<sup>1</sup> قسم الهندسة المدنية, جامعة النهريين, بغداد, العراق

<sup>2</sup> قسم الهندسة المدنية, الجامعة التكنولوجية, بغداد, العراق

<sup>3</sup> وزارة الموارد المائية, العراق

\*المؤلف المراسل: [mahmoud.s.al-khafaji@ced.nahrainuniv.edu.iq](mailto:mahmoud.s.al-khafaji@ced.nahrainuniv.edu.iq)

### الخلاصة

التغير بالمناخ يلعب دورا حاسما في تردد الاحداث المناخية المتطرفة و التي لها تأثيرات جسيمة على حالة الغطاء الأرضي. في هذه الورقة البحثية تم تقييم تماثل الغطاء الأرضي مع أنماط تردد الجفاف للظروف الحالية و المستقبلية في جابية حميرين في العراق. استخدمت بيانات نظام تحليل التنبأ بالمناخ في تحليل الطقس الشهرية و مؤشر تكرار حدوث الجفاف في جابية حميرين للفترة من 1984-2013. بالإضافة الى ذلك, فقد جرى تحليل الغطاء النباتي طبقا لصور الأقمار الصناعية. ان الاغطية النباتية المحسوبة من صور الأقمار الصناعية تم مقارنتها مع أنماط تردد الجفاف للتحري عن تأثير أنماط تردد الجفاف في الغطاء النباتي و توجه الغطاء النباتي. أشرت النتائج بان نمط الجفاف بسنتين او ثلاث سنوات جافة متتالية متبوعة بسنة واحدة رطبة قد هيمن في العقدين الماضيين على انماط تكرار الجفاف. علاوة على ذلك, ان الغطاء النباتي تناقص بنسبة 0.5% و 4.5% خلال المواسم الجافة و الرطبة على التوالي. الغطاء النباتي ممكن أن يعاد عندما تتابع سنة جافة بسنتين رطبة أو أكثر و تردد الجفاف يتناقص ب 23% و 28% خلال المواسم الجافة و الرطبة على التوالي. مع ذلك, عندما تهيم السنوات الرطبة فان الغطاء النباتي يزداد ب 1% و 37% خلال المواسم الجافة و الرطبة على التوالي. ان الجابية حساسة للتغير بالمناخ و ان الغطاء النباتي متعلق بشكل كبير بتردد الجفاف. ان مساحة الجفاف متوقع أن تزداد لتغطي معظم الجابية حتى عام 2049 نتيجة توابع التغير بالمناخ. ان الجفاف الموسمي يحتاج للمزيد من التحري في الدراسات المستقبلية.

**الكلمات المفتاحية:** الغطاء الارضي, تكرار الجفاف, التغيرات المناخية, حميرين

## 1. Introduction

During the last decades, rapid climate change was occurred due to global warming. This change is essentially caused by anthropic and natural actions. Climate change has a significant impact on the alteration of hydrological events, such as the streamflow and sediment yield, and can appear as a long-term drought followed by severe floods (Owor , et.al.,2009). Moreover, the frequency and severity of drought, were changed due to climate changes, and more extensive changes are expected to occur in the future, (Dai, 2012; McCarthy , et.al.,2001; Huete , et.al.,1999). In the upper part of the Tigris River's watershed in Turkey, precipitations decrease under the impact of climate change to 12.5% by 2021 and 26% by 2030 (Sen, 2018). In addition, the runoff will decrease to 30% after 2040. As Iraq is located in a semi-arid region. Therefore, the water resources of the Tigris River have been subjected to drought and pollution (Al-Ansari, 2016). For example, in southern parts of Iraq, severe droughts occurred from 2007 to 2009 followed by extreme short-term rainfall storms during a few months, with around two times the records (UN-ESCWA, 2020). The economic importance of vegetation cover (VC) is conducted to positive environmental role represented in protecting the soil from erosion, maintaining the moisture of the topsoil and encroachment of sand as well as supporting od food security, and standard of living (Marticorena , et.al.,1997). Monitoring of VC environments and potential temporal change in land cover (LC) is one of the main tools for assessing climate change and its environmental impacts, it is used to evaluate climate change and its impact on the VC environment time sequence of climatic elements and VC areas to analyse the vegetation pattern during a specific period (Al-Aroud , et.al.,2018). Droughts are classified into four categories: meteorological, agricultural, hydrological, and socioeconomic droughts (Zargar , et.al.,2011). For the spatiotemporal monitoring, and evaluation of these droughts over 150 indices, were developed and widely applied to assess the severity and extent of these droughts (Quiring, 2008). There are three methods usually used for monitoring and assessing the drought. These methods are a single index, multiple indices, and hybrid or composite indices (WMO and GWP, 2016). The Reconnaissance Drought Index (RDI) and Standardized Precipitation Index (SPI), are the commonly used simple drought indices when there is not sufficient soil moisture data (Wang , et.al.,2015). Often, drought frequency analysis is used to determine the exceedance probability, or return period of a drought of specific duration and/or severity (She , et.al.,2016). On another side, remote sensing techniques provide comprehensive

spatially, timely, and cost-effective information about LC. Several satellite-based vegetation indices are used to monitor and assess the quantity and quality of VC. The most efficient and commonly used satellite-based vegetation index is the Normalized Difference Vegetation Index (NDVI). This index is computed based on high spatial and temporal resolution digital images data, provided by several satellite sensors such as Landsat and Moderate Resolution Imaging Spectroradiometer (MODIS) (Storms and Hargrove, 2000; Peters, et.al.,2002; Eicic and Daniels, 1997; Morawitz, et.al.,2006; Lunetta, et.al.,2006). The advent of image processing techniques and geographic information systems (GIS) has increased the display, computing, maps overlaying, image stacking, and image classification as well as mapping and comparing various feature classes (WMO & GWP, 2016).

Diyala River is one of the five tributaries of the Tigris River. However, the streamflow suffered from a significant decrease and the sediment rates increased. In this river basin as well as in Tigris River Basin, a clear decrease in water resources was indicated. In the near future, additional deterioration and severe shortages in all water resources are expected (Al-Khafaji & Al-Chalabi, 2019; Adamo, et.al., 2018; Abbas, et.al.,2016). Hemrin Dam is one of the main hydraulic structures, in addition to Derbendikhan Dam, controlling the Diyala River Basin. It is located 120 km northeast of Baghdad. Hemrin Dam was constructed to control floods in the Diyala River and provide irrigation water for the Diyala Basin, which covers 300000 hectares of agricultural lands, as well as for electricity generation and developing fish wealth.

The main aim of this paper is to assess the meteorological drought and analysis of the drought frequency patterns (DFPs) and their effect on LC under climate change conditions in the Hemrin watershed. The novel method takes into consideration the statistical and satellite-based analysis of the interaction of land cover and drought.

## **2. Materials and Methods**

### **2.1 Study Area**

The Diyala River Basin is located in a semiarid region, of the Middle East between the latitudes 44.500° E and 46.833° E and the longitudes 33.216° N and 35.833° N. The watershed is divided between Iraq and Iran and has a total area of 32,600 km<sup>2</sup>, ~41% of which is in Iraq and the remaining part in Iran. Three dams have been built within the Iraqi part (Derbendikhan Dam,

Hemrin Dam, Diyala Weir) for multi-uses (Abbas , et.al., 2016). Hemrin Dam is an earth dam, constructed in the middle part of the Diyala River in 1981, about 120 km east of Baghdad for hydropower generation and irrigation, as part of the Khalus Irrigation Project. The total area of the Hemrin Dam Watershed is 12,822 km<sup>2</sup>, while 68% of its inside Iraq, and the remainder is in Iran. The total capacity of the Hemrin Reservoir is 2.4 BCM (Khassaf , et.al.,2009). The climate in the Hemrin watershed effect by the air from the Mediterranean Sea for periods from October to March which consider the rainy season, while from April to September the percentage of precipitation is 25-30% of the total annual precipitation (Al-Ansari, 1987).

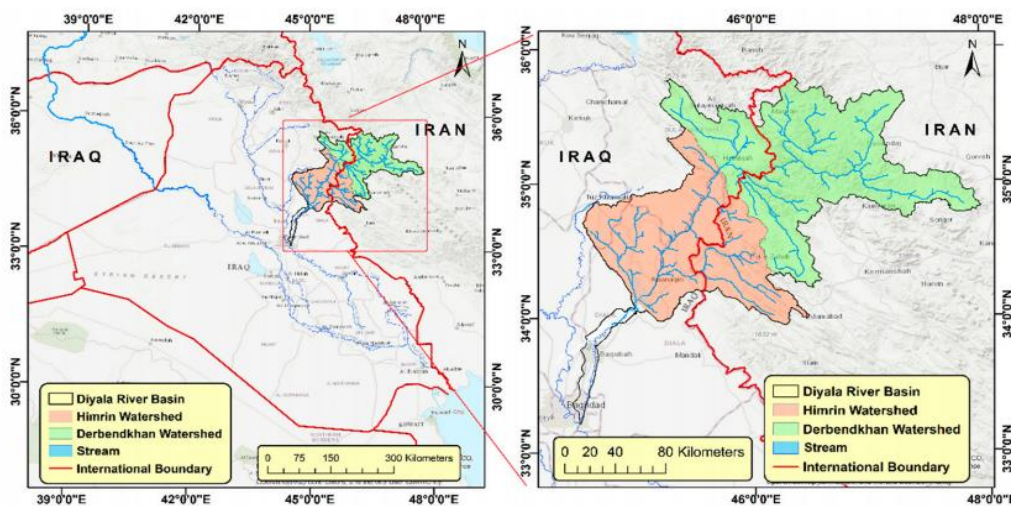


Figure (1) : Map of the Diyala River Basin (Al-Khafaji and Al-Chalabi, 2019).

Table (1) : Topographic characteristics of the Hemrin Watershed.

Topographic Character	Value
Total area (km <sup>2</sup> )	Extremely wet
Percentage of Iraqi Part (%)	Severely wet
Percentage of Iranian Part (%)	Moderately wet
Minimum ground elevation (m.a.s.l)	Near Normal
Maximum ground elevation (m.a.s.l)	Mild drought
Mean ground elevation (m.a.s.l)	Moderately drought
Minimum slope	Severe drought
Maximum slope	Extreme drought

## 2.2 Data Collection

In this paper, two types of weather data were used to calculate the RDI index. These data were monthly average temperatures and rainfall. These data were collected from CFSR. The CFSR

contains global weather data produced by the National Weather Service (NWS) and the National Centers for Environmental Prediction NCEP of the Global Forecast System for 30 years from 1984 to 2013.

For the computation of NDVI, a group of Landsat 7 and 8 images for the years 1989, 2000, 2011, and 2019 was used for both dry and wet seasons (downloaded from the USGS website (<http://earthexplorer.usgs.gov/>)). Figure (2) shows the input data of precipitation and potential evapotranspiration used to calculate the RDI index.

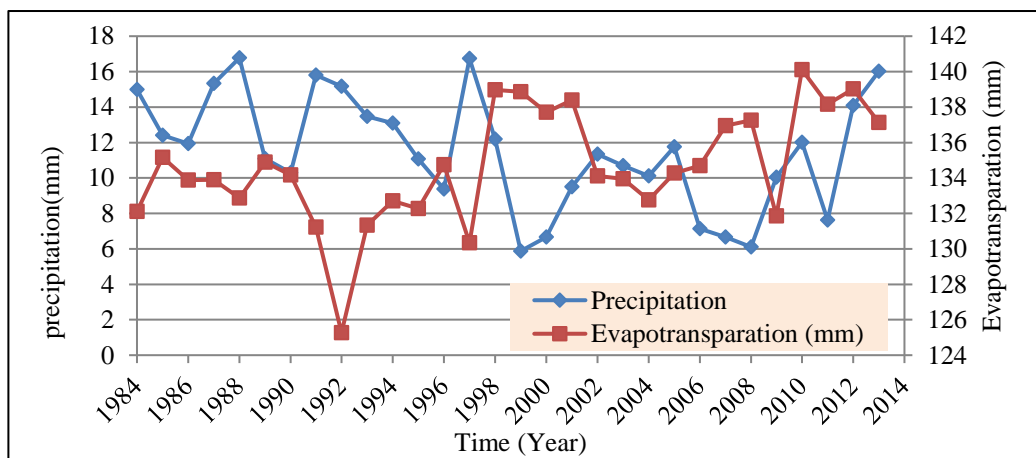


Figure (2) : Time series of precipitation and potential evapotranspiration with years for the period 1984-2013.

### 2.3 Methodology

The change in precipitation and surface air temperature were investigated for the period 1984-2013. Within this context, the meteorological drought of the study area was evaluated by calculating the Reconnaissance Drought Index (RDI). The cornerstone of this methodology was computing the average monthly RDI by using the DrinC software. This index was computed for the period 1984-2013 based on the Climate Forecast System Reanalysis (CFSR) weather data. In addition, the past climate precipitations and surface air temperatures were projected into future climate until 2050, based on scenario A2 using the climate model (gfdl\_cm2.1). This predicted weather data was used to compute the potential RDI of the study area. The computed RDI for the period 1984-2013 was used to perform a frequency analysis to determine droughts recurrence intervals and the exceedance probability and/or return periods of specific duration and/or severity. Moreover, remote sensing and geographic Information System (GIS) techniques were used to

determine the spatial and temporal change of LC within the study area for the considered period. Based on RDI, the meteorological drought was evaluated by determining the number of dry years (by taking the annual rate of RDI) as well as their frequency for two consecutive years and more, computing the return period for each occurrence and its exceedance probability and then assessing its effect on agricultural drought through the computation of VC based on evaluating the NDVI by using a group of four satellite images from the Landsat 7 and 8 sensors for the years 1989, 2000 and 2011. The image of 2019 was used to assess the accuracy of the dry areas computed from the CFSR data starting from the year 2014 using the climate model to assess the validity and reliability of climate model results.

The prediction of meteorological drought and VC for the future were obtained from the climate model (gfdl\_cm2\_1.1) for the period 2014 to 2050 to compute the spatial distribution of the RDI and DFPs. However, the potential VC areas for the years 2029, 2039, and 2049 were estimated by comparing the RDI values and drought frequency of the base period (1984-2013) with these of the period 2019-2050. The same percentages of increase and decrease in the VC for the base period were applied in 2019-2050.

## 2.4 Reconnaissance Drought Index (RDI)

Drought indices are indicators utilized to evaluate droughts and then its impacts. Traditionally these indices were applied to assess the drought severity. In the last four decades, many indices have been used. Recently, another index is presented for drought monitoring and assessment. This index is called Reconnaissance Drought Index (RDI) see Table 1, (Shah , et.al., 2013). The computation depends on precipitations and potential evapotranspiration. Precipitation alone cannot illustrate the effects of droughts on vegetation and agricultural production. Applying both precipitations and evapotranspiration in drought severity calculation and monitoring can increase the validity of the results (Gálya , et.al.,2017; Tran , et.al.,2017).

Based on the DrinC program, the value of the RDI drought index can be computed. DrinC provides a module for the computation of potential evapotranspiration (PET) with temperature-based methods: such as Hargreaves (Tmin, Tmax) (Hargreaves and Samani, 1981), Thornthwaite (Tmean) (Thornthwaite, 1948) and, Blaney – Criddle (Tmean) (Blaney and Criddle, 1950).

Hargreaves method (Eq.(1)) is used in this paper (because the available data was the maximum and minimum temperatures). The RDI is considered as to a more reliable index to assess drought in changing climatic environments (Tsakiris , et.al., 2007).

$$ET_o = 0.0023 (T_{max} - T_{min})^{0.5}(T_m + 17.8)R_a \quad (1)$$

where,  $T_m$ ,  $T_{max}$ , and  $T_{min}$  refer to: mean, maximum and minimum temperatures ( $^{\circ}C$ ); and  $R_a$  is the extraterrestrial radiation of the crop surface ( $MJm^{-2}day^{-1}$ ).

Based on the available monthly weather data, the annual average values of the RDI were determined. The positive values of this index refer to wet periods and negative values refer to drought periods, compared with the records. For the computation of the RDI on an annual basis, data may be either annual or monthly, while for computations on a seasonal basis (3 months, 6 months), monthly data is required.

Table (2) : Classification of RDI index (Shah et al., 2013).

RDI Values	Classification
2.0 or more	Extremely wet
1.5 to 1.99	Severely wet
1.0 to 1.49	Moderately wet
0 to 0.99	Near Normal
0 to -0.99	Mild drought
-1.0 to -1.49	Moderately drought
-1.5 to -1.99	Severe drought
-2 or less	Extreme drought

## 2.5 Return Period and Exceedance Probability

Many definitions were presented for specifying the return periods for different applications. Lloyd ,1970 , Loaiciga and Mariño (1991), and Shiau and Shen (2001) defined the return period as the average elapsed time between occurrences of critical events (i.e., floods or drought events). Some other authors, such as Vogel ,1987 , Bras ,1990, and Douglas , et.al., 2002, defined the return periods as the average number of trials required for the first occurrence of a critical event. In addition, Fernández ,1999 introduced an analytical approach for calculating the return period of drought events with a duration equal to or greater than a critical value for both Markov time-dependent and independent series based on a recursive algorithm proposed by Schwager (1983).

In this paper, the mean interval time, or average elapsed time, between two droughts events with a fixed severity or greater is adopted for computing the return period. The interval time (L) is the period from the beginning of the drought to the beginning of the next one, that is the sum of drought duration (L<sub>d</sub>) and non-drought duration (L<sub>n</sub>), illustrated in Figure (3) . However, the exceedance probability is computed from the law (1/return period).

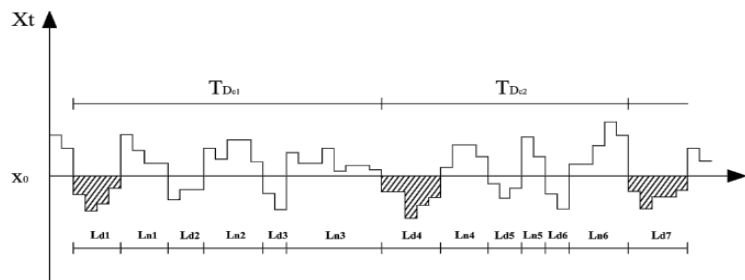


Figure (3): Interval (T<sub>Dc</sub>) between droughts with severity d<sub>c</sub> (represented by hatched area) (Bonaccorso et al., 2003).

## 2.6 Normalized Difference Vegetation Index (NDVI)

The NDVI is an index defined and developed by scientists at NASA’s Goddard Space Flight Center during the 1980s for monitoring the status of vegetation health, based on the difference between reflectance and absorption of green leaves in the near-infrared and red spectral bands (Tucker, 1979). The index value of each pixel was calculated by using;

$$NDVI = \frac{NIR-LR}{NIR+LR} \quad (2)$$

NIR ranges from (0.7 to 1.1) μm, while Red ranges from (0.58 to 0.68) μm. Normally, values of NDVI range from (-1 to +1) with +1 indicating healthy vegetation cover, and lower values representing stressed vegetation cover, and negative values representing open water, or high moisture content, respectively. The higher NDVI values are the healthier vegetation. The range value of NDVI in the wet seasons is much wider than in the dry seasons (Tran , et.al.,2017).

## 3. Results and Discussion

### 3.1 Computation of RDI and Drought Frequency Analysis

Figure (4) shows that the study area had undergone several drought intervals during the period from 1984 to 2013. During these intervals, the drought ranged between mild drought and near

normal. In the period 1984- 2000, ten mild droughts were computed with six times the frequency of two successive years. Whereas during the period 2000-2013 nine mild droughts were indicated with seven times the frequency of two successive years. However, two wet years were indicated in 2010 and 2012. Figure (5) shows the relationship between the drought (mild to extreme drought) successive reoccurrence interval and frequency as well as exceedance probability. The relationship of the recurrence of drought decreases with the increase in the period of drought. The recurrence of ten years happened once, and there is no recurrence of drought greater than it, unlike the two-year recurrence that is common to occur during this period.

The frequency of drought recurrence with two successive years of mild drought is the most occurring and common in the base period followed by three successive years, and then a large value of droughts periods (from four to ten successive mild droughts) occurred less. This recurrence of drought is due to the strong fluctuation of precipitation, see Figure (3) , it decreased for several years and then increased. Thus, this decrease is accompanied by an increase in the values of potential evapotranspiration.

Maps shown in Figure 6 represent spatial distributions of RDI for the years 1989, 2000, and 2011 for both dry and wet seasons (the reason for choosing these years, in line with the satellite imagery taken for these years, is to compare the drought areas with the VC areas. Its values range from -0.99 to 1.06 (mild drought to moderate wet). Droughts were identified in the region for 6 months (for wet and dry seasons), and types of drought were categorized based on index classifications see Table (2).

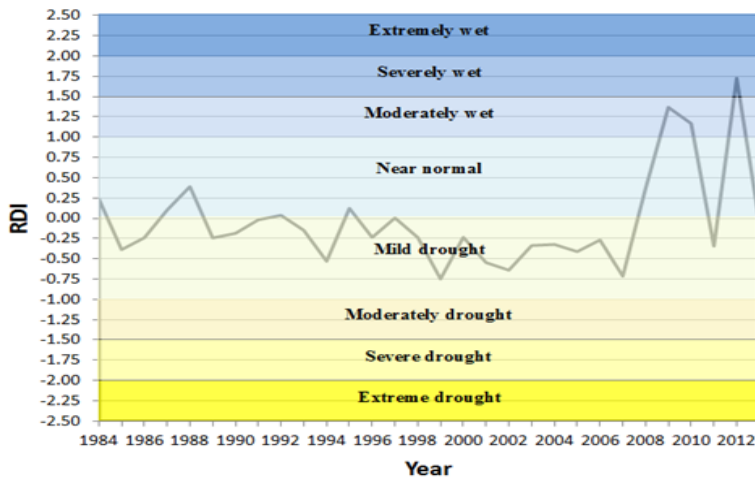


Figure (4): RDI for the base period 1984-2013.

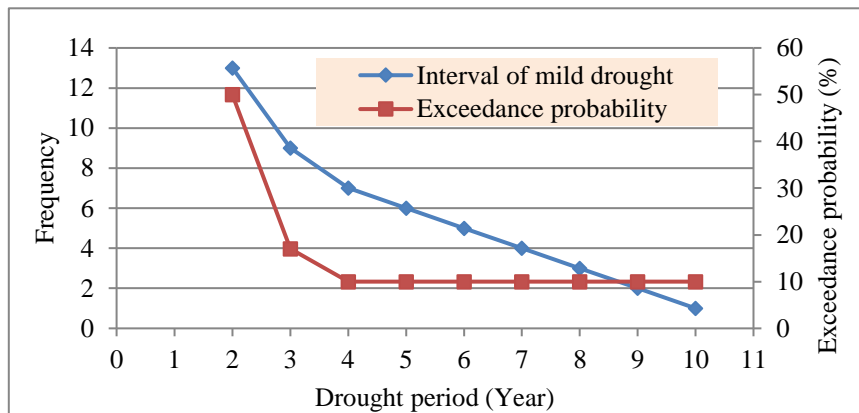


Figure (5): Drought (Mild to extreme drought) successive reoccurrence interval versus frequency and exceedance probability, for the base period 1984 to 2013.

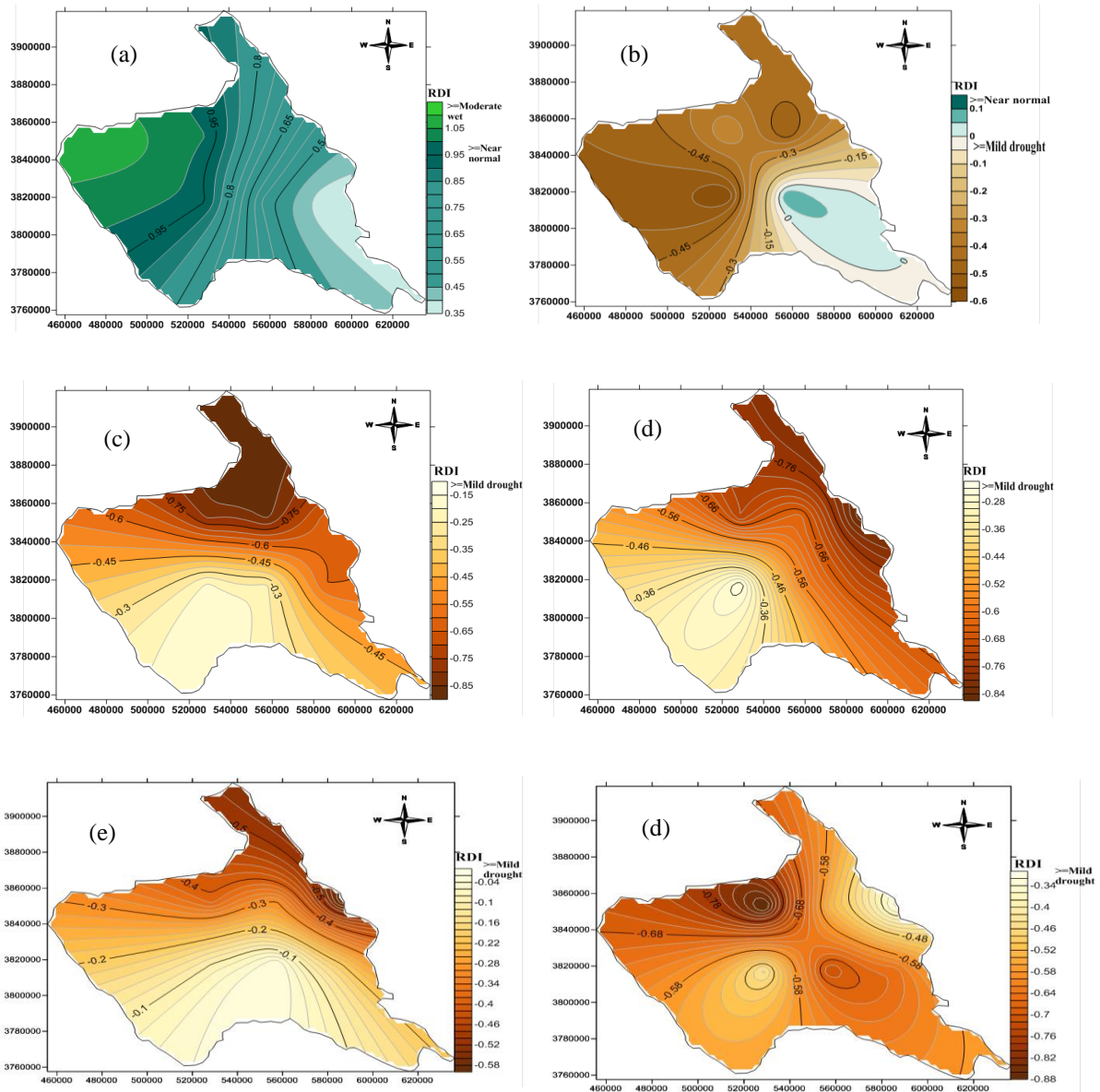


Figure (6): Distribution of drought for periods 1984, 2000, and 2011 (a, b, c, d, e, and f respectively) for both seasons wet and dry, (a) 1989 wet season, (b) 1989 dry season, (c) 2000 wet season, (d) 2000 dry season, (e) 2011 wet season and (f) 2011 dry season.

In the wet season of the year 1989, the value of the RDI ranged between near normal and moderate wet. In this season, the wetness increases towards the west of the region. However, in the dry season, the drought was near normal with an RDI value range between 0 and 0.1 on the

southeastern side whereas a mild drought spread within more than two-thirds of the watershed area (covered 10563 km<sup>2</sup> from the watershed area) and its intensity increases especially toward the western and northern sides. For the years 2000 and 2011, the whole area of the watershed was covered by drought for both dry and wet seasons. The drought intensity increases towards the north, northeast, and east.

### 3.2 Computation of NDVI

Figure (7) shows the distribution of NDVI for the wet and dry seasons of these years, (the green color on the map in Figure 7 indicates VC). The areas of VC in the dry and wet seasons during the considered years are listed in Table 4. The VC area in the wet season for the years 2000 and 2011 is less than that of the dry season. The reason for this is that the precipitations were reduced for the fourth, fifth, and sixth months. In addition, the potential evapotranspiration in these months was not very high. The period extending from 1989 to 2000 was dry. It affected the type of VC and changed it to be summer plants, this case remained until 2011. The same type of plants continued as the period is also dry. It is worth to noticed that the RDI is a climate index that refers to dry areas but these dry areas don't need to be free of VC. However, there may be dry areas but they contain VC since the RDI does not mean that these areas are absolutely arid. It also refers to wet areas, but wet areas don't need to contain a VC, sometimes there are plants, and sometimes not.

The VC in the period 1989-2000 decreased from 0.76% to 0.27% (64.30% of the initial VC) of the total area of the watershed in the dry season and from 4.85% to 0.08% (98.30% of the initial VC) in the wet season. The reason for this decrease is the effect of eight dry years with only three wet years. The arrangement of these years every two or three dry years is followed by a wet year. As for the period 2000-2011, the VC decreased from 0.27% to 0.16% (41.12% of the initial VC) of the total area of the watershed, and from 0.08% to 0.02% (70.90% of the initial VC) in the dry and wet seasons respectively. Unlike the previous period, the wet years were between the dry years and this is why it decreased by 23% in the dry and 28% in the wet season. This is consistent with the results of the computed RDI during these periods. Where the result of RDI indicates a long

period of dry compared to a short period of wet, the result of NDVI indicates a decrease in the area of VC during this period as shown in Table (3).

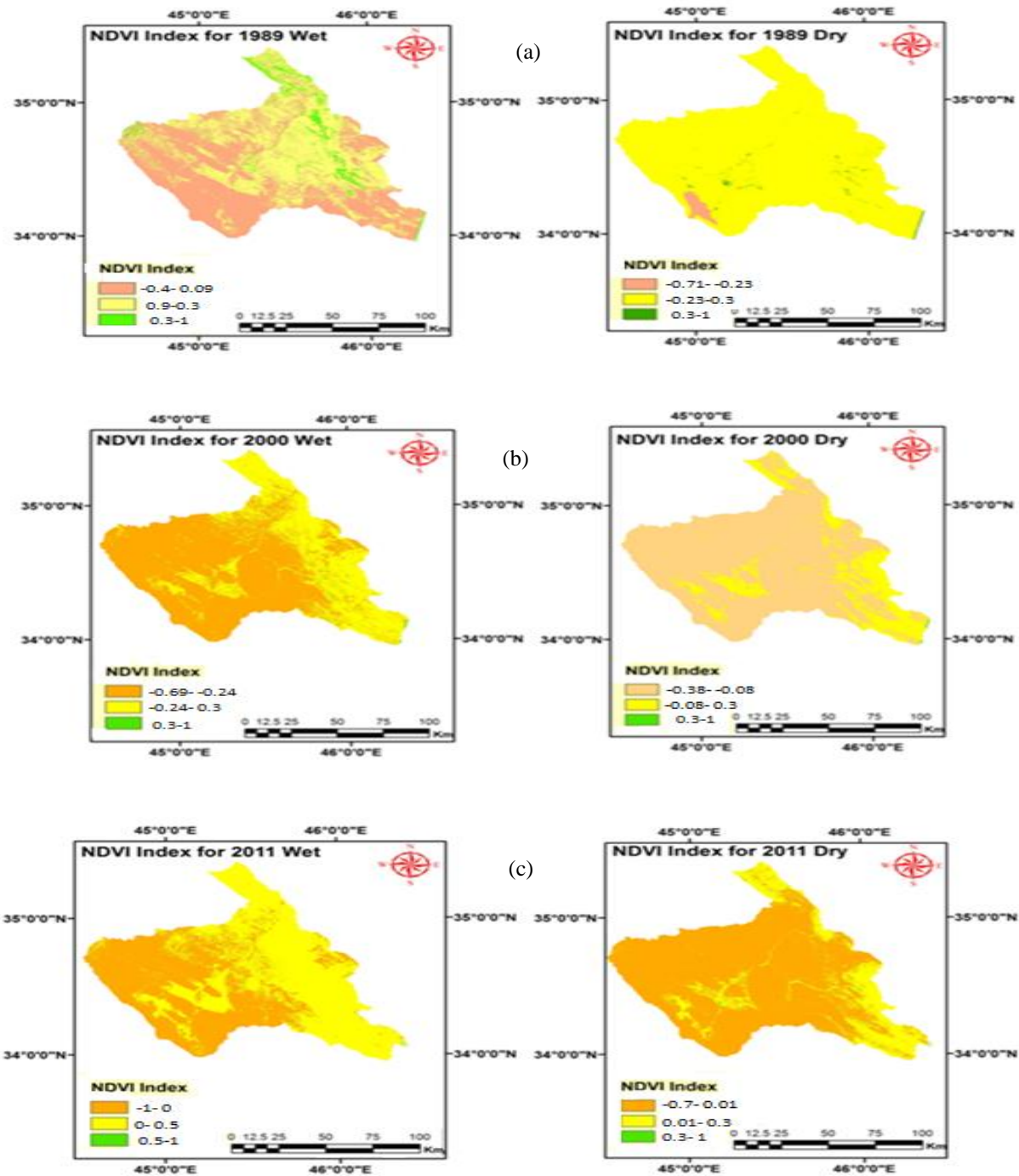


Figure (7) : Distribution of NDVI for the years 1989, 2000, and 2011 (a, b, and c respectively) for the dry and wet seasons.

Table (3) : VC areas of the years 1989, 2000, and 2011 for both dry and wet seasons.

Years	Area (km <sup>2</sup> )	
	Dry season	Wet season
1989	97.45	621.48
2000	34.79	10.58
2011	20.46	3.08

Figures (8 and 9) show the areas of VC compared to the areas of drought covering the watershed in the dry and wet seasons, it can be noticed that with the increase of drought areas the percentage of VC areas decreases and vice versa. In the dry season of the year 1989, the dry area covers 82% of the watershed while it decreases to 26% in the wet season. The VC was 0.8% and 5% from the area of a watershed for the dry and wet seasons respectively, while the years 2000 and 2011 are covered by 100% drought and VC was 0.3% and 0.2% for the dry season and 0.08% and 0.02% from the watershed area for the wet season respectively.

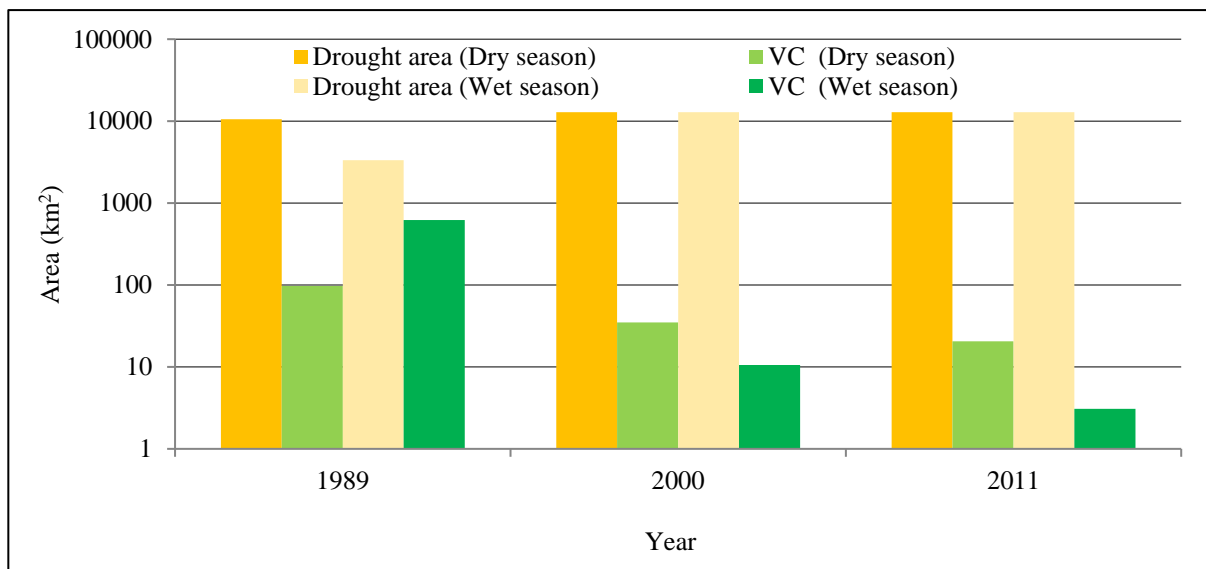


Figure (8): Drought and VC areas in the dry and wet seasons.

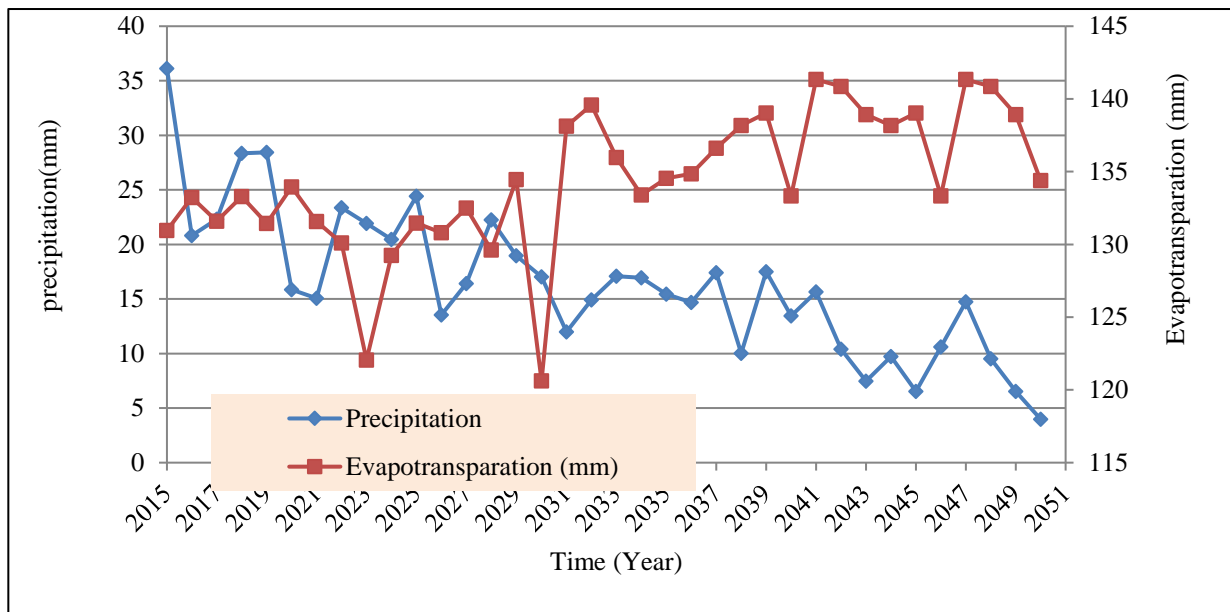


Figure (9): Expected precipitation and potential evapotranspiration for the period 2015-2050.

### 3.3 Effect of Climate Change on Drought Frequency

The monthly weather data (surface air temperatures and precipitation), for the period 2014 to 2050 was projected using the climate model (gfdl\_cm2\_1.1) based on the monthly average CFSR weather data, for the entire base period (1984-2013) as shown in Figure 9. The figure indicates the expected decrease in the amount of precipitation during the period (2014-2050). This in turn increases drought and reduces the VC for the future.

Based on the obtained future climate data, the RDI for the period 2014-2050 was computed by the DrinC program, see Figure 10. The RDI analysis showed that the period 2014- 2019 is a little dry and most years are near historical records. Recurrence is recorded twice in two successive years 2017, 2018, and 2019. However, in the period 2020-2030, the least dry period occurs. These years witnessed near-normal drought for the years 2022, 2024, and 2026, as well as in the year 2023 it was extremely wet and moderately wet for the year 2029. The period 2030-2050 tends to be drier, while, in 2037 and 2039 near normal and all remaining years are mild droughts. The reason for this drought is the severe decrease in amounts of precipitation and increase in potential evapotranspiration.

Figure (11), illustrates an inverse relationship between drought frequency and drought period, which is similar to the relationship in the base period. Whereas, the difference between the base and future periods is that the number of occurrences of droughts for successive years is slightly greater, especially for the period 2030-2050. However, the recurrence of drought every two years is more frequent and more common which can be observed every four years occurrence with a probability of 25%, but the base period occurs approximately every two years. From Figure (10) , the potential RDI distribution indicated that the values of RDI ranged between 1.06 to -1.5 (moderate wet to moderate drought). For the year 2019, moderate wet was distributed in one-third of the watershed area and intensity increased towards the west, while the near normal spread over the remaining part, for the dry season more than 90% of the area was covered by mild drought, the wet areas turned dry during this season. In the year 2029 of the wet season, the RDI values ranged between near normal and moderate wet, while in the dry season, it was about 99% of the area of the mild drought and 10% was near normal. For the year 2039, the wet season, the value of the index ranged between -0.25 to 0.99. However, the area near normal covered more than two-thirds of the area of the region and increased towards the northwest and southeast, while in the dry season, the entire area was covered by mild drought and increased towards the south. In the year 2049, its wet season is covered by mild drought, more than 97%, the rest is near normal, and in the dry season, RDI ranged between the moderate drought that increases from the center towards the north, east and south of the region, and the mild drought, it starts from the middle to the west. The expected drought areas are listed in Table (5) .

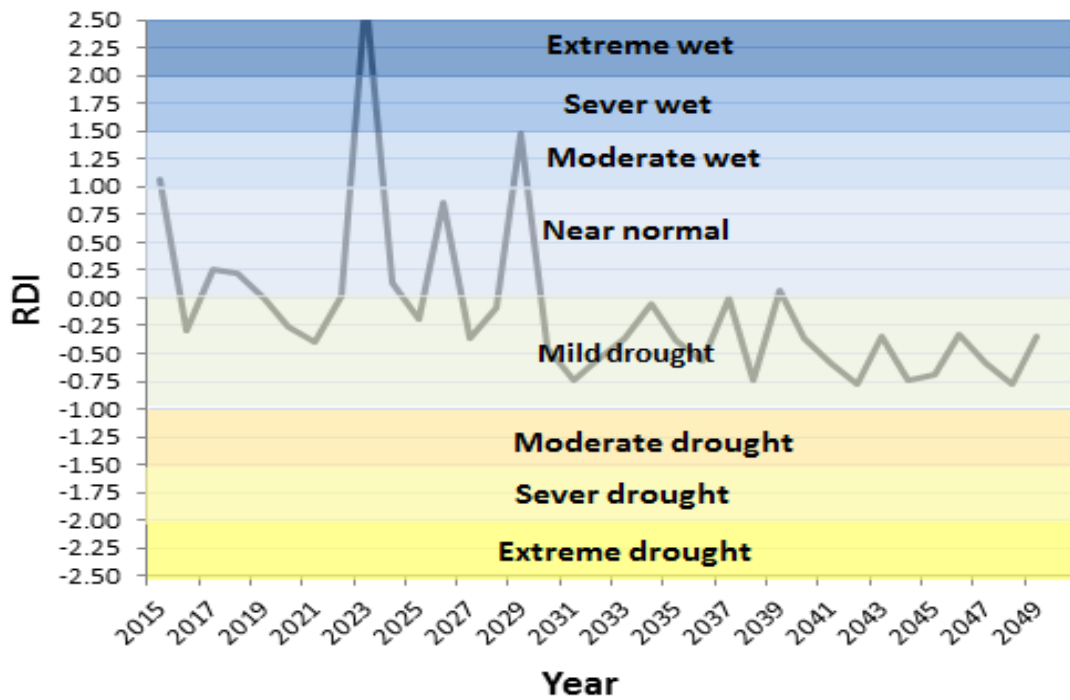


Figure (10): Predicted RDI for the period 2014- 2050.

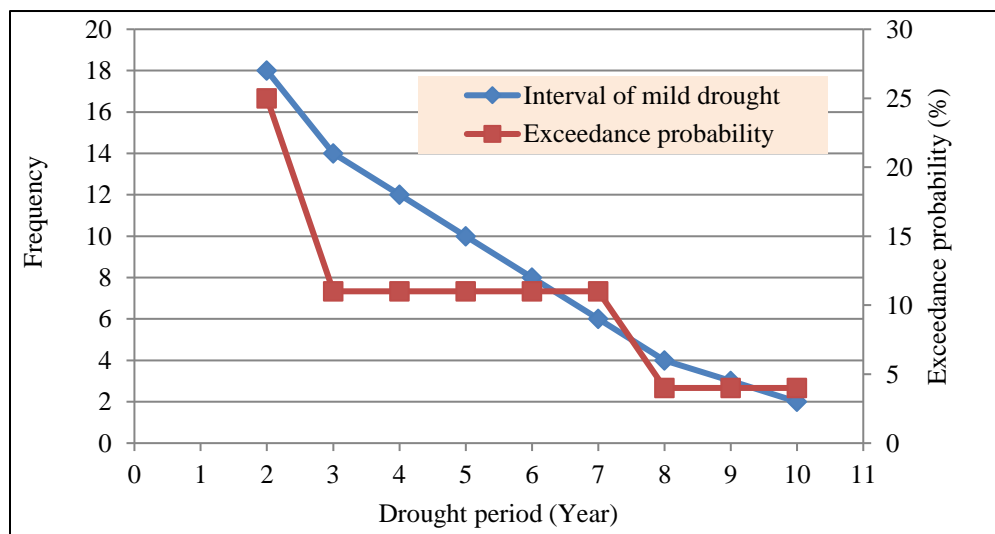


Figure (11): Expected Drought (Mild to extreme drought) successive reoccurrence interval versus frequency and exceedance probability, for the period 2014-2050.

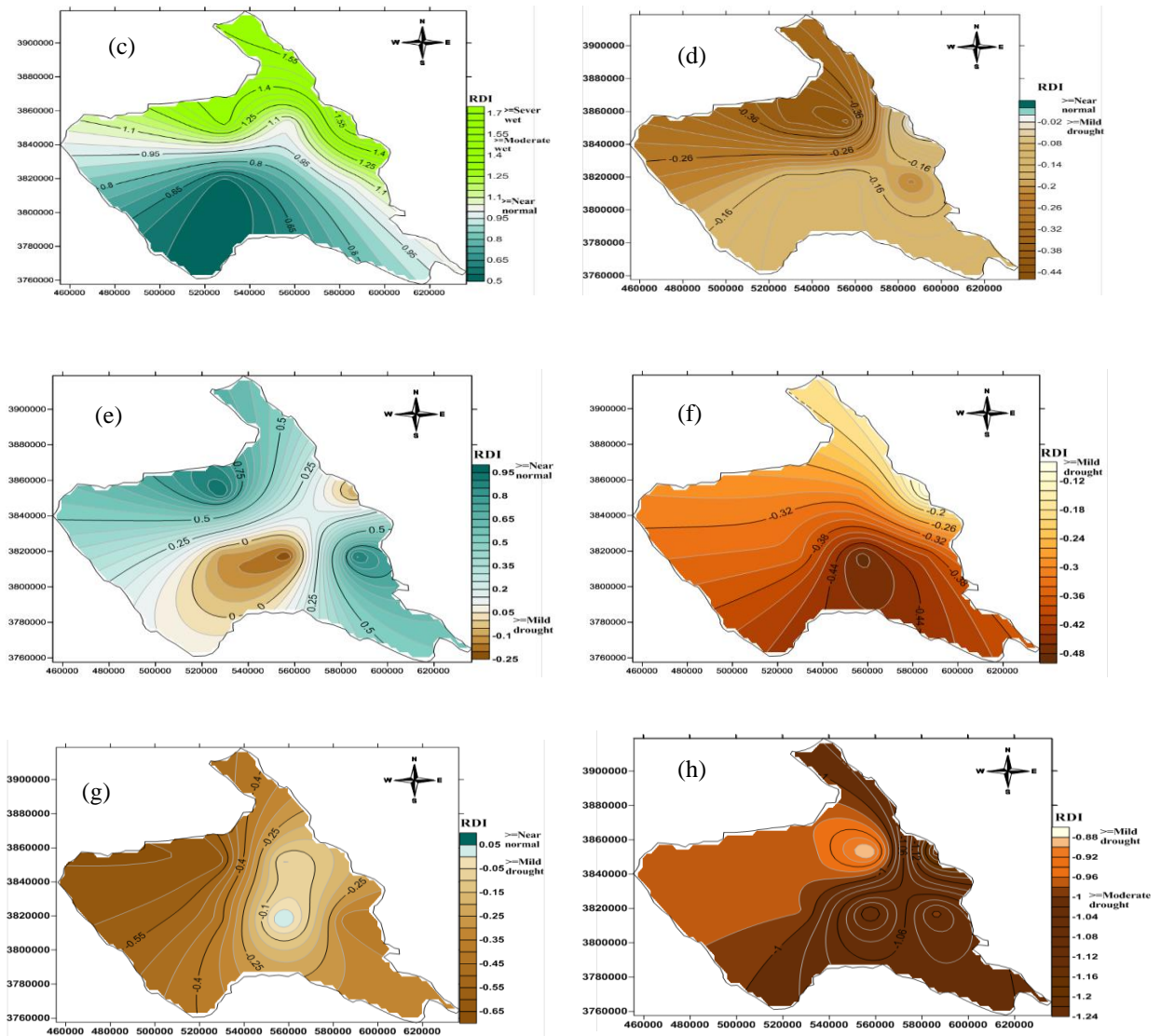


Figure (12) : Distribution of drought wet and dry. (a) 2019 wet season, (b) 2019 dry season, (c) 2029 for the wet season, (d) 2029 for the dry season, (e) 2039 for the wet season, (f) 2039 for the dry season, (g) 2049 for the wet season and (h) 2049 for the dry season.

Table (5): Potential drought areas for the years 2019, 2029, 2039, and 2049.

	Area (km <sup>2</sup> )	
	Dry season	Wet season
2019	11958	0
2029	12822	0
2039	12822	3000
2049	12822	12156

### 3.4 Effect of Climate Change on Vegetation Cover

The VC for the period 1989-2011 was tracked through the NDVI index that was derived from the Landsat satellite images, Figure (13), showing the distribution of LC for the year 2019 for dry and wet seasons), as well as climate changes were evaluated during this period and the region was shown to be very sensitive to climate changes. When the RDI recorded more dry periods than wet periods and a high frequency of drought, the results of NDVI indicate a high decrease in the area of VC, as for the period 1998-2000 (which is 98.30% of the initial VC in the wet season and 64.30% of the initial VC in the dry season).

For the future, the impact of climate change on the LC was predicted based on the estimated RDI values utilizing the gfdl-cm2-1.1climate model data, which started in 2014. The computed RDI values for the base period (1984-2013), which were based on the CFSR data, and the predicted RDI values for the future (2014-2050), which were based on the gfdl-cm2-1.1climate model data, show that the period 2011-2019 was a very wet period, with seven wet years and only two dry years. Computed NDVI of the year 2019 shows that the VC increased from 0.16% to 1.00% (611% of the initial VC of the total area of the watershed) and from 0.02 % to 38.00 % (155857% of the initial VC) in the dry and wet seasons respectively. This proves that this period was really wet. This agrees with the results of the predicted RDI distribution for the future which is highly similar to that of the base period. This supports the certainty of using the gfdlcm2-1.1climate model data. The values of VC for the years 2029, 2039, and 2049 were predicted by comparing these years with the base period in terms of RDI values and results of DFPs in these periods.

The period 2019-2029 is very similar to the period 2011-2019, where 2023 is extremely wet, 2029 is moderately wet and RDI values of other years are very close. Therefore, the VC of 2029 was increased with the same VC increase percent of the period 2011-2019 for both wet and dry seasons, as listed in Table (6). Also, the RDI values and dry years number and frequency of the

period 2029-2039 are somewhat similar to that of the period 1989-2000. Therefore, the VC area decreased by a percentage of 65 % and 98 % for the dry and wet seasons, respectively, of the year 2039. However, the period 2039-2049 is successive dry years. Consequently, the VC area of the dry season decreases with a percentage of 87 %. This percent is calculated by adding the decreased percent of VC for the case of seven successive dry years followed by three wet years (65%) to the effect of three wet years (23 %). Whereas, the VC of the wet season decreased with a percent of 126 %, which is the result of adding the decreased percent of VC for the case of seven successive dry years followed by three wet years (89%) to the effect of three wet years (28 %).

Figure (14) illustrates the predicted dry and VC areas covering the watershed. It is expected that the areas of drought increase and VC decreases to be covered all the watershed areas in 2049. In 2019, the estimated drought (VC) percentage is approximately 93% (1%) and 0% (38%) for both dry and wet seasons respectively. While the year 2029 is covered by drought for the dry seasons by 100% and decreased to 0% in the wet season, these percentages correspond to areas of VC of 8% and more than 99% respectively, from the area of the region. While the VC is reduced to 2% and 3% against 100% dry areas and 23% for the dry season and the wet season for the year 2039 and the VC continues to decrease until it reaches 0% in the year 2049 in the wet season, a dry area covering 95% of the area of the watershed.

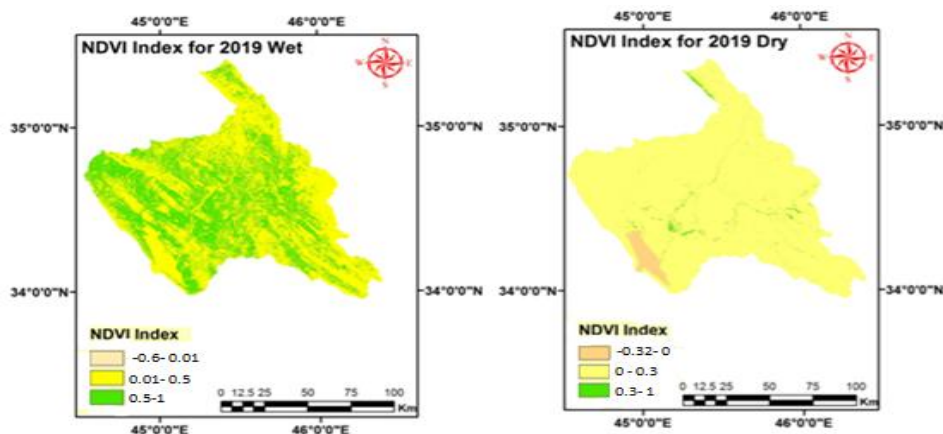
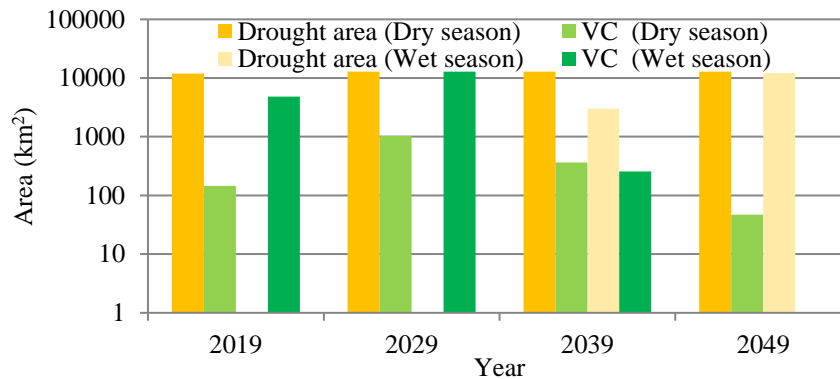


Figure (13): Distribution of LC for the year 2019 for the dry and wet seasons.

Table (6): VC areas for the years 2019, 2029, 2039, and 2049.

Years	Area (km <sup>2</sup> )	
	Dry season	Wet season
2019	146	4806
2029	1035	12822
2039	362	256
2049	47	0

Figure (14): Predicted drought and VC areas of dry and wet seasons for the years 2019-2050.



#### 4. Conclusion

The effect of climate change on the spatiotemporal patterns of drought frequency and the response of land cover (LC) to this change in Hemrin Watershed, Iraq was investigated. The RDI was computed utilizing the DrinC software based on data downloaded from CFSR weather data. In addition, the NDVI was derived from four satellite images of Landsat 7 and 8 for the years 1989, 2000, 2011, and 2019. Results of RDI and NDVI for the period 1984-2013 showed that the arrangement of dry and wet years greatly affects the VC. Consecutive dry years followed by successive wet years reduce the effect of drought on the VC area by 23% in the dry season and by 28% in the wet season. A comparison of NDVI-based VC and the computed RDI based on the climate model data (gfdl-cm2-1.1model) for the year 2019 showed that the climate model gave good and reliable results. For the future period (2014-2050), matching the predicted drought spatial distributions with that of the base period showed that most of the watershed regions would not remain dry or wet constantly, but they change throughout the seasons of the years according to the

climatic conditions. Satellite-based investigation of VC for the year 2019 indicated that VC increased from 0.16 % to 1.00 % (611% of the initial VC) of the total area of the watershed) and from 0.02% to 38.00% (155857% of the initial VC) in the dry and wet seasons respectively. This indicates that the period 2011-2019 was wet and agreed with the CFSR data of the period 2011-2013. Predicted VC of the period 2014-2050 showed that climate change causes a severe increase in the interval and frequency of the successive dry years. Consequently, in the study area, the VC is vulnerable and significantly decreases to the increase in the drought periods and frequency.

**Acknowledgements** Thanks and sincere gratitude to the technical and faculty staff of the Department of Civil Engineering at the University of Technology-Iraq, for their valuable support and scientific assistance. Also, gratitude and thankfulness to the Ministry of Water Resources, Iraq, for their assistance in conducting the field investigations and providing the data.

## References

- Owor, M., Taylor, R.G., Tindimugaya, C., & Mwesigwa, D. (2009). Rainfall intensity and groundwater recharge: empirical evidence from the Upper Nile Basin. *Environmental Research, Letters* 4: 035009. <https://doi.org/10.1088/1748-9326/4/3/035009>
- Dai, A. E. (2012). Drought under global warming: a review. *Wiley Interdisciplinary Reviews: Climate Change* 3: 617-617. <https://doi.org/10.1002/wcc.190>
- McCarthy, J.J., Canziani, O.F., Leary, N.A., Dokken, D.J., & White, K.S. (2001). *Climate change 2001: impacts, adaptation, and vulnerability: contribution of Working Group II to the third assessment report of the Intergovernmental Panel on Climate Change. (Vol. 2)*. Cambridge University Press. <https://doi.org/10.1002/joc.775>
- Huete, A. J., Haverkamp, C., & Van Leeuwen, W. (1999). MODIS vegetation index (MOD 13) algorithm theoretical basis document version 3, University of Arizona, 1200.
- Sen, Z. (2018). Climate Change Expectations in the Upper Tigris River Basin, Turkey. *Theoretical and Applied Climatology*, 137: 1–17. <http://dx.doi.org/10.1007/s00704-018-2694-z>
- Al-Ansari, N. (2016). Hydro-politics of the Tigris and Euphrates basins. *Eng.*, 8: 140-172. <https://doi.org/10.4236/eng.2016.83015>
- UN-ESCWA (2020). *Inventory of Shared Water Resources in Western Asia*. <https://www.unescwa.org/publications/inventory-shared-water-resources-western-asia>. Accessed 26 November 2020.

Prince, S.D. (1991). A model of regional primary production for use with coarse resolution satellite data. *Int J of RS*, 12: 1313-1330.

Haverkamp, S., Fohrer, N., & Frede, H.G. (2005). Assessment of the effect of land-use pattern on hydrologic landscape functions: a comprehensive GIS-based tool to minimize model uncertainty resulting from spatial aggregation *Hydro Process*, 19 , pp. 715-727

Marticorena, B., Bergametti, G., Gillette, D., & Belnap, J. (1997). Factors controlling threshold friction velocity in semiarid and arid areas of the United States. *J of Geophy Res: Atm*, 102(D19): 23277-23287. <https://doi.org/10.1029/97JD01303>

Al-Aroud, A.M., AL-Balisi, H.H., & Al-Ghanmien, T.M. (2018). Modern climatic modifications on the plant cover in the Wadi Araba North Basin. *The Jordanian J of Social Sci*, 11: 30-47.

Zargar, A., Sadiq, R., Naser, B., & Khan, F.I. (2011). A review of drought indices. *Environmental Reviews*, 19(NA): 333-349. <https://doi.org/10.1139/a11-013>

Quiring, S.M. (2009). Monitoring drought: an evaluation of meteorological drought indices. *Geogr Compass*, 3: 64–88. <http://dx.doi.org/10.1111/j.1749-8198.2008.00207.x>

World Meteorological Organization (WMO) and Global Water Partnership (GWP) (2016). *Handbook of Drought Indicators and Indices* (M. Svoboda and B.A. Fuchs). Integrated Drought Management Programme (IDMP), Integrated Drought Management Tools and Guidelines Series 2, Geneva.

Wang, H., Rogers, J.C. & Munroe, D.K. (2015). Commonly used drought indices as indicators of soil moisture in China. *J of Hydrometeorology*, 16: 1397-1408. <https://doi.org/10.1175/JHM-D-14-0076.1>

She, D., Mishra, A.K., Xia, J., Zhang, L., & Zhang, X. (2016). Wet and dry spell analysis using copulas. *Int J of Clim*, 36: 476-491. <https://doi.org/10.1002/joc.4369>

Stoms, D.M., & Hargrove, W.W. (2000). Potential NDVI as a baseline for monitoring ecosystem functioning. *Int J of RS*, 21: 401-407. <https://doi.org/10.1080/014311600210920>

Peters, A.J., Walter-Shea, E.A., Ji, L., Vina, A., Hayes, M., & Svoboda, M.D. (2002) Drought monitoring with NDVI-based standardized vegetation index. *Photo. Eng and RS*, 68: 71-75.

Ecic, F.L., & Daniels, E. (1997). Land-cover changes in sub-Saharan Africa (1982–1991): application of remotely sensed surface temperature and vegetation indices at a continental scale. *Remote Sens Env*, 61: 181-200.

Morawitz, D.F., Blewett, T.M., Cohen, A., & Alberti, M. (2006). Using NDVI to assess vegetative land cover change in central Puget Sound. *Environmental monitoring and assessment*, 114: 85-106. <https://doi.org/10.1007/s10661-006-1679-z>

Lunetta, R.S., Knight, J.F., Ediriwickrema, J., Lyon, J.G., & Worthy, L.D. (2006). Land-cover change detection using multi-temporal MODIS NDVI data. *RS of Env*, 105: 142-154. <https://doi.org/10.1016/j.rse.2006.06.018>

Al-Khafaji, M.S., & Al-Chalabi, R.D. (2019). Assessment and mitigation of streamflow and sediment yield under climate change conditions in Diyala River Basin, Iraq. *Hydrology*, 6(3), 63; <https://doi.org/10.3390/hydrology6030063>

Adamo, N., Al-Ansari, N., Sissakian, V., Knutsson, S., & Laue, J. (2018). Climate change: consequences on Iraq's environment. *J Earth Sci Geotech Eng*, 8: 43–58.

Abbas, N., Wasimi, S., & Al-Ansari, N. (2016). Impacts of climate change on water resources in Diyala River Basin. *Iraq J of Civil Eng and Arch*, 10: 1059-1074. <https://doi.org/10.17265/1934-7359/2016.09.009>

Shah, R., Manekar, V.L., Christian, R.A., & Mistry, N.J. (2013). Estimation of Reconnaissance Drought Index (RDI) for Bhavnagar District, Gujarat, India. *International Journal of Environmental and Ecological Engineering* , 7: 507 -510.

Gálya, B., Blaskó, L., Jóvér, J., Kovács, G., & Tamás, J. (2017) 15<sup>th</sup> Int. Conf. on Environmental Science and Technology (Rhodes / Greece).

Tran, H.T., Campbell, J.B., Tran, T.D., & Tran, H.T. (2017). Monitoring drought vulnerability using multispectral indices observed from sequential remote sensing (Case Study: Tuy Phong, Binh Thuan, Vietnam). *GI Sci and R S*, 54: 167-184. <https://doi.org/10.1080/15481603.2017.1287838>

Hargreaves, G.H., & Samani, Z.A. (1982). Estimating potential evapotranspiration. *J of the Irr and Drai Eng*, 108: 225-230.

Thornthwaite, C.W. (1948). An approach toward a rational classification of climate. *Geographical review*, 38: 55-94. <https://doi.org/10.2307/210739>

Blaney, H.F., & Criddle, W.D. (1950). Determining water requirements in irrigated areas from climatological and irrigation data. *Washington Soil Conservation Service*, 48: 126-147.

Tsakiris, G., Pangalou, D., & Vangelis, H. (2007). Regional drought assessment based on the Reconnaissance Drought Index (RDI). *WARM*, 21: 821-833. <https://doi.org/10.1007/s11269-006-9105-4>

Lloyd, E.H. (1970). Return periods in the presence of persistence. *J of Hydro*, 10: 291-298. [https://doi.org/10.1016/0022-1694\(70\)90256-8](https://doi.org/10.1016/0022-1694(70)90256-8)

Loaiciga, H.A., & Mariño, M.A. (1991). Recurrence interval of geophysical events. *J of Water Res Plan and Man* 117: 367-382.

Shiau JT, & Shen HW (2001). Recurrence analysis of hydrologic droughts of differing severity. *J of Water Res Plan and Man* 1991, 127: 30-40. [https://doi.org/10.1061/\(ASCE\)0733-9496\(2001\)127:1\(30\)](https://doi.org/10.1061/(ASCE)0733-9496(2001)127:1(30))

Vogel, R.M. (1987). Reliability indices for water supply systems. *J of Water Res Plann and Man*, 113: 563-579. [https://doi.org/10.1061/\(ASCE\)0733-9496\(1987\)113:4\(563\)](https://doi.org/10.1061/(ASCE)0733-9496(1987)113:4(563))

Bras, R.L. (1990). *Hydrology: An Introduction to Hydrologic Science*. Addison-Wesley Publishing Company, Boston, USA, 643 pp.

Douglas, E.M., Vogel, R.M., & Kroll, C.N. (2002). Impact of streamflow persistence on hydrologic design. *J of Hydro Eng*, 7: 220-227. DOI: 10.1061/(ASCE)1084-0699(2002)7:3(220)

Fernández, B., & Salas, J.D. (1999). Return period and risk of hydrologic events. I: mathematical formulation. *J of Hydro Eng*, 4: 297-307. [https://doi.org/10.1061/\(ASCE\)1084-0699\(1999\)4:4\(297\)](https://doi.org/10.1061/(ASCE)1084-0699(1999)4:4(297))

Schwager, S.J. (1983). Run probabilities in sequences of Markov-dependent trials. *J of the A Stat Assoc*, 78: 168-175.

Bonaccorso, B., Cancelliere, A., & Rossi, G. (2003). An analytical formulation of return period of drought severity. *Stochastic Environmental Research and Risk Assessment*, 17: 157-174. <https://doi.org/10.1007/s00477-003-0127-7>

Tucker, C.J. (1979). Red and photographic infrared linear combinations for monitoring vegetation. *R S of Env*, 8: 127-150. [https://doi.org/10.1016/0034-4257\(79\)90013-0](https://doi.org/10.1016/0034-4257(79)90013-0)

Khassaf, S.I., Al-Adili, A.S., & Rasheed, R.S. (2009). Seepage analysis underneath Diyala weir foundation. In *Proceedings of the Thirteen International Water Technology Conference, IWTC, Hurghada, Egypt*: 12-15.

Al-Ansari, N. (1987). Geological and hydrological investigation of Hemrin reservoir. *J of Water Res*, special publication No.2.